TISSUE ENGINEERING: Part A
Volume 21, Numbers 5 and 6, 2015

DOI: 10.1089/ten.tea.2014.0189

Transforming Growth Factor Beta 1 Augments Calvarial Defect Healing and Promotes Suture Regeneration

Sameer Shakir, BS,[1] Zoe M. MacIsaac, MD,[1] Sanjay Naran, MD,[1] Darren M. Smith, MD,[1] Michael R. Bykowski, MD,[1] James J. Cray, PhD,[2] Timothy K. Craft, BA,[3] Dan Wang, DMD,[4] Lee Weiss, PhD,[5] Phil G. Campbell, PhD,[6] Mark P. Mooney, PhD,[4] Joseph E. Losee, MD,[1] and Gregory M. Cooper, PhD[1]

Background: Repair of complex cranial defects is hindered by a paucity of appropriate donor tissue. Bone morphogenetic protein 2 (BMP2) and transforming growth factor beta 1 (TGFβ1) have been shown separately to induce bone formation through physiologically distinct mechanisms and potentially improve surgical outcome for cranial defect repair by obviating the need for donor tissue. We hypothesize that a combination of BMP2 and TGFβ1 would improve calvarial defect healing by augmenting physiologic osteogenic mechanisms.
Methods/Results: Coronal suturectomies (3 × 15 mm) were performed in 10-day-old New Zealand White rabbits. DermaMatrix™ (3 × 15mm) patterned with four treatments (vehicle, 350 ng BMP2, 200 ng TGFβ1, or 350 ng BMP2 + 200 ng TGFβ1) was placed in suturectomy sites and rabbits were euthanized at 6 weeks of age. Two-dimensional (2D) defect healing, bone volume, and bone density were quantified by computed tomography. Regenerated bone was qualitatively assessed histologically. One-way analysis of variance revealed significant group main effects for all bone quantity measures. Analysis revealed significant differences in 2D defect healing, bone volume, and bone density between the control group and all treatment groups, but no significant differences were detected among the three growth factor treatment groups. Qualitatively, TGFβ1 treatment produced bone with morphology most similar to native bone. TGFβ1-regenerated bone contained a suture-like tissue, growing from the lateral edge of the defect margin toward the midline. Unique to the BMP2 treatment group, regenerated bone contained lacunae with chondrocytes, demonstrating the presence of endochondral ossification.
Conclusions/Significance: Total healing in BMP2 and TGFβ1 treatment groups is not significantly different. The combination of BMP2 + TGFβ1 did not significantly increase bone healing compared with treatment with BMP2 or TGFβ1 alone postoperatively at 4 weeks. We highlight the potential use of TGFβ1 to regenerate calvarial bone and cranial sutures. TGFβ1 therapy significantly augmented bony defect healing at an earlier time point when compared with control, regenerated bone along the native intramembranous ossification pathway, and (unlike BMP2 alone or in combination with TGFβ1) permitted normal suture reformation. We propose a novel method of craniofacial bone regeneration using low-dose, spatially controlled growth factor therapies to minimize potentially harmful effects while maximizing local bioavailability and regenerating native tissues.

Introduction

Congenital anomalies and traumatic injuries involving the pediatric craniofacial skeleton continue to pose significant reconstructive challenges. Underlying dural tissues allow for complete calvarial reossification in children less than 2 years of age; however, this osteogenic capacity diminishes in an age-dependent manner.[1–4] A child's dura mater loses its potential to spontaneously heal large osseous deficiencies after 2 years of age,[5–9] while split-thickness calvarial grafts, the gold standard for treatment of large calvarial defects, cannot be reliably harvested until the child's diploic space matures at ~10 years of age.[10] Consequently, there is a subset of pediatric patients who have a need for alternative reconstructive therapies. Autogenous bone grafts harvested from the ribs or iliac crest are unappealing due to significant donor site morbidity and limited tissue yield in this pediatric population.[11] Bone substitutes,

[1]Department of Plastic Surgery, University of Pittsburgh, Pittsburgh, Pennsylvania.
[2]Department of Oral Health Sciences, Medical University of South Carolina, Charleston, South Carolina.
Departments of [3]Anthropology and [4]Oral Biology, University of Pittsburgh, Pittsburgh, Pennsylvania.
[5]The Robotics Institute, Carnegie Mellon University, Pittsburgh, Pennsylvania.
[6]Institute for Complex Engineered Systems, Carnegie Mellon University, Pittsburgh, Pennsylvania.

including alloplastic materials (polymethylmethacrylate, porous polyethylene, and hydroxyapatite), cadaveric bone grafts, and demineralized bone matrix, have significant drawbacks. These materials are incompatible with the growing craniofacial skeleton, susceptible to infection, and lack comparable effectiveness to autogenous bone.[11,12] To circumvent the inadequacies of these presently available approaches, emerging tissue engineering applications aim to repair bony craniofacial defects through osteoinduction.

Several studies have been published on calvarial reconstruction using various growth factor- and stem cell-based tissue engineering therapies.[13–23] For example, off-label use of recombinant human bone morphogenetic protein 2 (BMP2) for craniofacial reconstruction has been studied and even translated into the clinical setting.[24–26] This powerful osteoinductive agent, however, is fraught with complications[27–31] and delivers variable success.[32] Not only are supraphysiologic doses utilized to achieve osseous closure but current BMP2 therapies may also pose significant risks to the patient, including significant neurologic complications, male sterility, seroma formation, increased inflammatory infiltrates, and heterotopic ossification.[33–37] In addition to BMP2, exogenous applications of recombinant human transforming growth factor beta 1 (TGFβ1) promote bone formation through recruitment and proliferation of osteoblasts at the calvarial defect site.[38–42] However, limited studies have been performed to evaluate the efficacy of this growth factor in calvarial defect healing. Our laboratory has developed a methodology of inkjet-based bioprinting capable of delivering low-dose, spatially controlled growth factor therapies.[43] Development of alternative osteogenic therapies will benefit from an improved understanding of regenerated bone biology before tissue engineering therapies can rival autogenous bone-based treatment modalities. The present study aims to assess the efficacy of printing low-dose osteogenic growth factors (BMP2 and TGFβ1) in addressing calvarial regeneration in a neonatal leporine model. We hypothesized that a combination of BMP2 and TGFβ1 would significantly improve calvarial defect healing compared with either growth factor used alone.

Materials and Methods

Sample

Twenty-seven wild-type New Zealand White rabbits (*Oryctolagus cuniculus*) were utilized in this study, with a total of 54 right and left coronal sutures as independent samples. All rabbits were born into the breeding colony at the University of Pittsburgh in the Department of Anthropology vivarium. This study was reviewed and approved by the University of Pittsburgh Institutional Animal Care and Use Committee. Rabbits were chosen without regard to sex due to the species' minimal sexual dimorphism.[44] Rabbits were assigned randomly to one of five treatment groups: (1) suturectomy with empty defect, which served as the surgical control group ($n=14$ sutures); (2) suturectomy with non-printed (200–400 μm) thick DermaMatrix™ (Synthes) derived from acellular dermal matrix (ADM) ($n=10$) to serve as the vehicle control; (3) suturectomy with 350 ng BMP2 patterned on ADM ($n=10$); (4) suturectomy with 200 ng TGFβ1 patterned on ADM ($n=10$); and (5) suturectomy with a combination of 350 ng BMP2 and 200 ng TGFβ1 patterned on ADM ($n=10$). Each rabbit received two randomized treatments (right and left side of the suturectomy defect site). Patterns were rinsed with sterile PBS to remove unbound proteins for 24 h before implantation. Notches were cut into the patterns to maintain orientation before implantation. Growth factor bioinks were printed on ADM using our custom two-dimensional (2D) bioprinting system, based on a piezoelectric inkjet printhead (30-mm diameter orifice) from MicroFab Technologies. Patterning materials and methodology were previously described.[43]

Surgery

Coronal suturectomies were performed as previously described.[45] At 10 days of age, all rabbits were anesthetized with an intramuscular (IM)[32] injection (0.59 mL/kg) of a solution consisting of 91% Ketaset (ketamine hydrochloride, 100 mg/mL; Aveco Co., Inc.) and 9% Rompun (xylazine, 20 mg/mL; Mobay Corp.). The scalps were then shaved, depilated, and prepared for surgery. The calvariae were exposed using a midline scalp incision, and the skin reflected laterally to the supraorbital borders. All animals received postoperative IM injections (2.5 mg/kg) of Baytril (Bayer Corp.) as a prophylaxis for infection. A 3-mm-long by 15-mm-wide strip of frontal and parietal bones, including the entire length and width of the coronal suture, was extirpated and removed in one piece from pterion to pterion using a cutting burr. Care was taken to preserve the meningeal (fibrous) layer of the dura mater and the regional vascularity (Fig. 1).

Rabbits in the control group received a suturectomy only. The periosteal and skin incisions were then closed with 4-0 resorbable Vicryl sutures (Ethicon). For rabbits in the other four groups, the suturectomy sites were treated with 3-mm-long by 15-mm-wide DermaMatrix implants from one of the four treatment groups described above. Growth factors were purchased from R and D Systems, each diluted in 10 mM sodium phosphate, pH 7.4, and printed with a custom inkjet printer onto the ADM for final concentrations of 350 ng/mL (BMP2) or 200 ng/mL (TGFβ1). Following ADM placement, the periosteal and skin incisions were repaired as above.

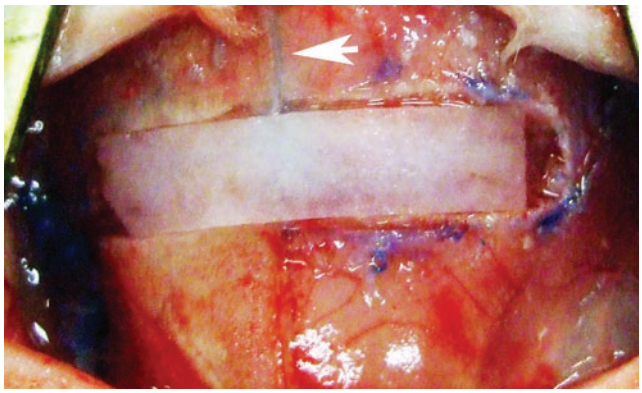

FIG. 1. Intraoperative image depicting 3×15 mm coronal strip suturectomy. Note the sagittal suture bisecting the ADM into two equal halves. Each half received one of four possible treatments or nothing. Left lower corner of the ADM is notched for purposes of orienting the biopatterned surface. ADM, acellular dermal matrix. Color images available online at www.liebertpub.com/tea

Data collection

At 42 days of age, 23 rabbits were euthanized ($n=46$ sutures) with an IV (40 mg/kg) injection of pentobarbital (Nembutal; Abbott Laboratories). An additional sample of four control rabbits ($n=8$ sutures) who received empty suturectomies was euthanized at 126 days of age to assess for defect healing at this later time point. Skull specimens were harvested anteriorly across the orbits, posteriorly through the occipital protuberance, and laterally through the parietal bones. Tissues from the defect regions of the calvariae were fixed in 10% buffered neutral formalin (Sigma).

Microcomputed tomography analysis

Microcomputed tomography (Micro-CT; Siemens Inveon Micro-CT) and subsequent three-dimensional (3D) reconstructions of the CT data (Amira 3.1; Mercury Computer Systems) were performed on explants of the surgical sites to assess the architecture of regenerated bone. The computed tomographic[8] scans were analyzed with OsiriX image processing software (Kanteron Systems) to assess the defect area, bone volume, and bone density. CT scans containing the postrendering artifact or folded pattern placement were excluded from defect area healing, volume, and density analyses.

Means and standard errors for defect areas were calculated and compared among the five treatment groups using a one-way analysis of variance (ANOVA). Significant intergroup differences were assessed using the least significant difference multiple comparison test. All data were analyzed using SPSS 21.0 for Macintosh (SPSS, Inc.). Differences were considered significant if $p \le 0.05$.

Two-dimensional percent defect healing

CT scans were rendered in 8.09 mm thick transverse sections of the rabbit calvariae. The sagittal suture served as the medial edge of each right and left-sided defect, which extended 7.5 mm laterally. Radiolucent regions within the defects were included in the overall defect area measurements. ''Defect area percent healing'' was determined by the following equation: $\frac{measured\ defect\ area - control\ defect\ area}{control\ defect\ area} \times 100$, where control defect area was the mean of the measured control defect area values.

Regenerated bone volume

CT scans were simultaneously rendered in 126.37 μm thick sagittal and coronal fields of view. The sagittal suture served as the medial edge for right and left-sided treatments placed within the suturectomy sites. In the sagittal field of view, a 3 mm length within the original defect margin served as the region of interest (ROI) for measuring regenerated bone volume. This ROI was extrapolated to a total width of 7.5 mm from the midline to represent the original right and left-sided defect margins centered along the sagittal suture. Pixels within the ROI with a value greater than or equal to −200 were considered bone. This threshold value was utilized across all samples. Three-dimensional growth segmentation of the bone within the ROI rendered a calculated bone volume.

Regenerated bone density

CT scans were simultaneously rendered in 126.37 μm thick sagittal and coronal fields of view. Similar to volume calculations, a ROI measuring 3×7.5 mm from the sagittal suture midline was obtained. Pixels outside of this ROI were cropped out. The lower and upper limits for 3D growth segmentation of bone within the ROI were set to −200 and 9999, respectively, rendering a calculated bone density. To control for individual variability in CT image intensity, each calculated bone density was represented as a percentage of its corresponding native bone density. This native bone density was obtained from each CT scan. Regenerated bone density was determined from the following equation: $\frac{measured\ density - native\ bone\ density}{native\ bone\ density} \times 100$.

Histological analysis

Tissues from the defect regions of the calvariae were decalcified with 10% ethylenediaminetetraacetic acid (Sigma), dehydrated in a series of alcohol washes, and embedded in paraffin for histologic analysis. The specimens were then sectioned in the coronal plane at a thickness of 5 μm and stained with Harris hematoxylin (Surgipath Medical Industries) and eosin Y (Ricca Chemical Company) or Russell-Movat's pentachrome (American Master-Tech Scientific, Inc.) to assess bone morphology using conventional, qualitative bright-field light microscopy.

Results

CT analysis

Two-dimensional percent defect area healing. Percent healing measured from CT in the surgical control animals ($n=5$ sutures) was 0.00% ± 9.87% (mean ± standard error); 40.17% ± 14.39% in vehicle-treated animals ($n=10$); 72.13% ± 7.98% in BMP2-treated animals ($n=10$); 88.84% ± 5.71% in TGFβ1-treated animals ($n=8$); and 83.13% ± 8.85% in BMP2 + TGFβ1-treated animals ($n=8$). Figure 2 depicts a representative CT composite of defect healing across the treatment groups. One-way ANOVA revealed a significant group main effect ($F=9.479$, $p<0.001$). Least significant difference (LSD) *posthoc* analysis for multiple

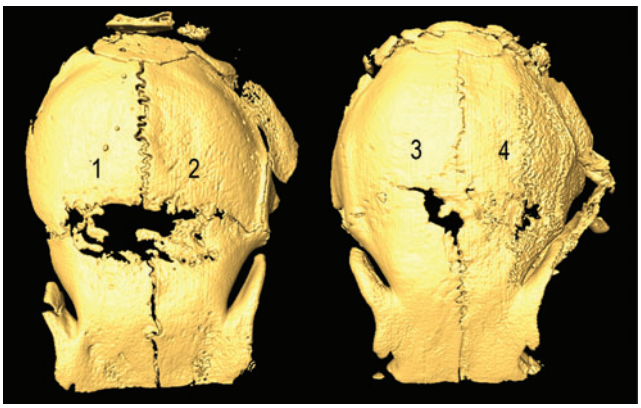

FIG. 2. CT representation of 2D defect healing across experimental groups. (1) Vehicle, (2) 350 ng BMP2, (3) 200 ng TGFβ1, (4) 350 ng BMP2 + 200 ng TGFβ1. Note improved linear 2D defect healing with the three biopatterned growth factor therapies. 2D, two-dimensional; BMP2, bone morphogenetic protein 2; CT, computed tomography; TGFβ1, transforming growth factor beta 1. Color images available online at www.liebertpub.com/tea

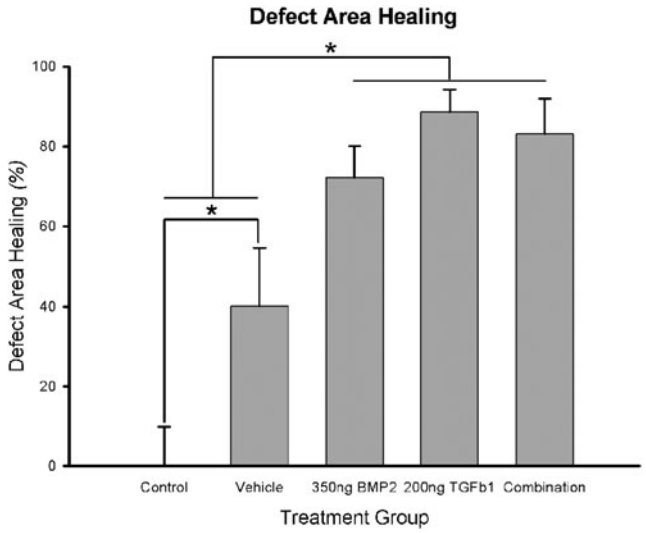

FIG. 3. Quantitative linear 2D defect healing across treatment groups. *Statistical significance ($p < 0.05$). Defect healing in vehicle treatment was significantly better than healing in control. Defect healing in biopatterned growth factor therapies was significantly better than healing in vehicle treatment. However, defect healing among biopatterned growth factor therapies was not significantly different.

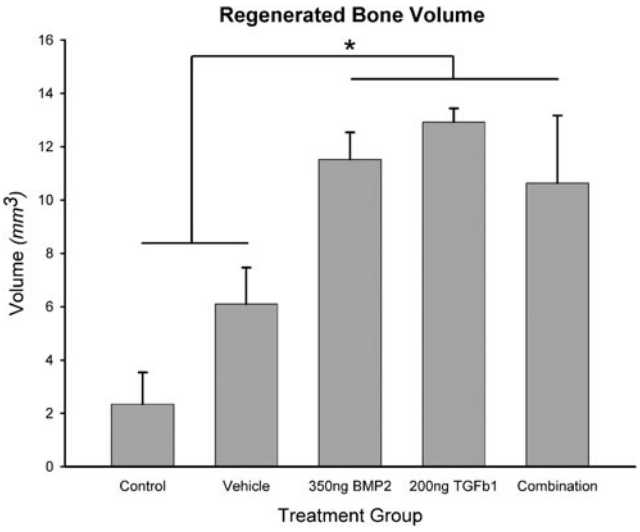

FIG. 4. 3D CT quantitative representation of regenerated bone volume within original defect margins. *Statistical significance ($p < 0.05$). Regenerated bone volumes were significantly greater in biopatterned growth factor therapy groups compared with control and vehicle treatment. There was no statistically significant difference in regenerated bone volumes between control and vehicle treatment.

comparisons revealed significant differences between the control group and all treatment groups, including vehicle, 350 ng BMP2, 200 ng TGFβ1, and 350 ng BMP2 + 200 ng TGFβ1, $p < 0.05$. Defect healing in vehicle-treated animals was significantly different when compared with the three growth factor-treated groups, $p < 0.05$, but no significant differences were detected among these three treatment groups (Fig. 3).

Regenerated bone volume. Bone volume measured from CT in control animals ($n = 4$ sutures) was $2.34 \pm 1.20\,mm^3$; $6.10 \pm 1.36\,mm^3$ in vehicle-treated animals ($n = 6$); $11.52 \pm 1.02\,mm^3$ in BMP2-treated animals ($n = 6$); $12.93 \pm 0.51\,mm^3$ in TGFβ1-treated animals ($n = 4$); and $10.64 \pm 2.53\,mm^3$ in BMP2 + TGFβ1-treated animals ($n = 4$). One-way ANOVA revealed a significant group main effect ($F = 8.695, p < 0.001$). LSD *posthoc* test for multiple comparisons revealed significant differences between control animals and growth factor-treated animals, $p < 0.05$. *Posthoc* analysis revealed no significant differences between regenerated bone volumes in control versus vehicle-treated animals ($p = 0.079$). *Posthoc* analysis also revealed significant differences between vehicle-treated animals and growth factor-treated animals, but no significant differences were detected among the three growth factor-treated groups (Fig. 4).

Regenerated bone density. Bone density (as a percentage of native bone density) measured from CT in control animals ($n = 4$ sutures) was $97.14\% \pm 6.85\%$; $74.61\% \pm 5.80\%$ in vehicle-treated animals ($n = 6$); $68.23\% \pm 6.61\%$ in BMP2-treated animals ($n = 6$); $63.67\% \pm 3.24\%$ in TGFβ1-treated animals ($n = 4$); and $60.83\% \pm 4.09\%$ in BMP2 + TGFβ1-treated animals. One-way ANOVA revealed a significant group main effect ($F = 18.766$, $p < 0.001$). LSD *posthoc* analysis for multiple comparisons revealed significant differences between measured bone densities in control animals compared with all other treatments. Bone densities were significantly different between vehicle and BMP2 + TGFβ1 combination treatments ($p = 0.044$). There was no significant difference in the bone density between the control treatment and native bone ($p = 0.626$). No significant differences in bone densities were detected among the three growth factor-treated groups (Fig. 5).

Histological analysis

Bone regeneration. Hematoxylin and eosin stain revealed variable tissue regeneration across groups (Fig. 6). Control and vehicle-treated defects primarily contained fibrous tissue spanning the defect margins with minimal amounts of bone regeneration (labeled FT in Fig. 6A). BMP2-regenerated bone contained lacunae with chondrocytes, demonstrating the presence of endochondral ossification (purple stain in Fig. 6B) and also appeared thicker than native bone with more marrow spaces (Fig. 6B). Movat's pentachrome stain further demonstrated cartilage in the BMP2-regenerated bone by staining these mucins green (green stain/asterisk in Fig. 7B). This cartilage intermediate was not present in any other groups (Fig. 7). Lamellar bone formation, which was present across all growth factor treatment groups, appears as a darker red stain within predominantly yellow-stained woven bone (red stain in Fig. 7B–D). The TGFβ1 treatment group produced bone with cellularity and matrix density most similar to native bone. Overall, bone regeneration primarily occurred along defect margins, although bone was also present within the ADM parenchyma (asterisks in Fig. 6). Regenerated bone vascularity, as qualitatively observed, appeared to be grossly consistent across the three growth factor treatment groups.

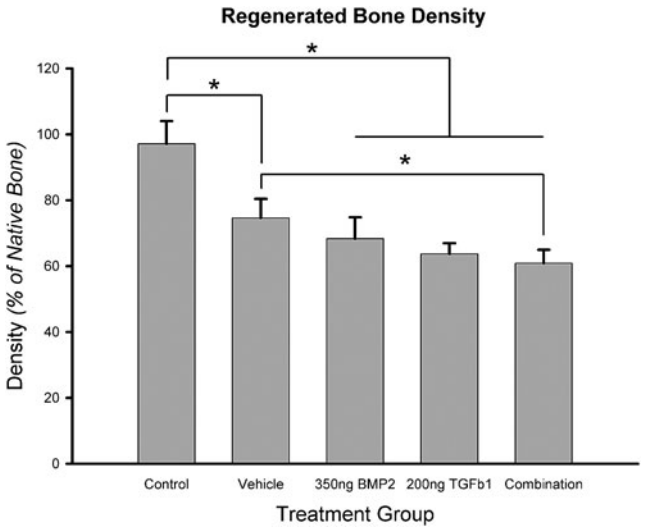

FIG. 5. Quantification of regenerated bone density based on 3D CT analysis. *Statistical significance ($p<0.05$). Densities are reported as a percentage of native bone density, which was measured from calvarial bone posterior to the original defect site. Regenerated bone density in all treatment groups was significantly lower than in control. There was no statistically significant difference in regenerated bone density among biopatterned treatment groups. Combination treatment produced bone with a significantly lower density than vehicle treatment.

Suture regeneration. Interestingly, TGFβ1-regenerated bone contained a suture-like tissue, growing from the lateral edge of the defect margin toward the midline. This neocoronal suture had vascularized, interdigitating collagen fibers with bone edges containing a zone of horizontally ordered osteoblasts (Fig. 8 bottom panels). Newly formed bone was maintained at a fixed distance from the neocoronal suture. This suture-like tissue was not present in any other groups at the 6-week time point. 18 weeks postoperatively, control rabbits appeared to regenerate previously resected sagittal and coronal sutures as determined by histological and CT data (Fig. 8 upper panels and Fig. 9, respectively). Defects were not completely healed at this later time point.

Discussion

There is considerable necessity for improved approaches to craniofacial bone regeneration in the pediatric population. While distant autogenous grafts (e.g., rib, iliac crest) are available, they provide limited tissue and come at the expense of significant discomfort and wound-related morbidity. Local autogenous grafts are largely unavailable until later in childhood when a diploic space develops.[46] Alloplastic implants are not compatible with the growing craniofacial skeleton and are at risk of infection and extrusion.[11] BMP2 and other growth factor-based strategies offer an exciting alternative, but the incompletely understood biological profiles of these powerful morphogens with local effects on sutural fusion and neural development[31] as well as systemic effects throughout an organism cannot be ignored.[47–58] We propose a novel method of craniofacial bone regeneration using low-dose, spatially controlled growth factor therapies to minimize potentially harmful effects of these growth factors while maximizing their local bioavailability.

The neonatal rabbit model utilized in this study correlates with the immature pediatric craniofacial skeleton, providing an optimal *in vivo* context for analyzing various growth factor-based therapies.[59] We observed similar linear 2D defect closure across growth factor treatment groups in our neonatal rabbit model. These data suggest that the application of low-dose BMP2 and TGFβ1, in isolation or in combination, induces healing in immature craniofacial bone defects postoperatively at 4 weeks.

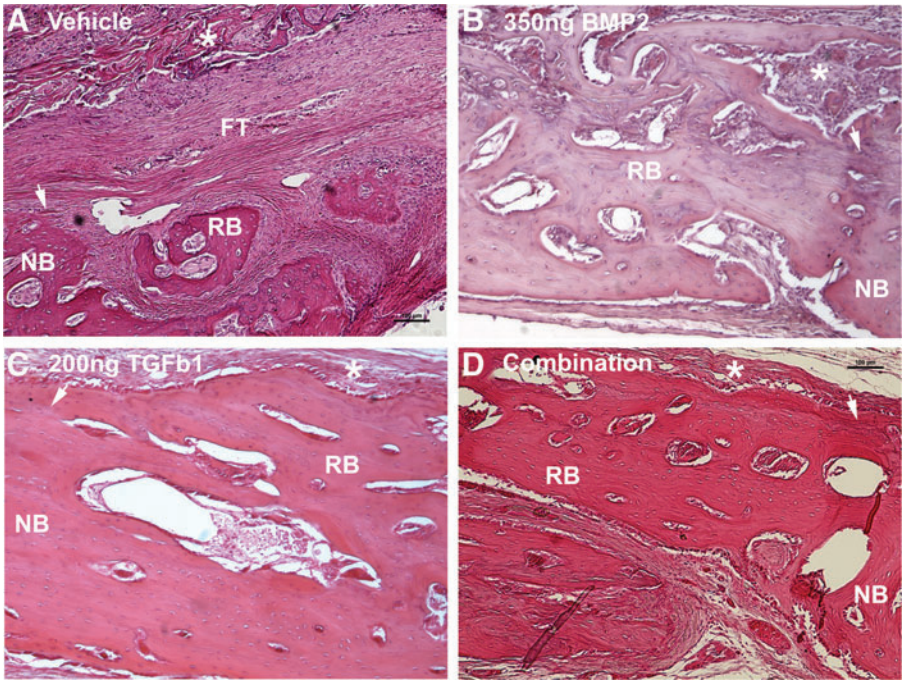

FIG. 6. Hematoxylin and eosin composite of regenerated bone across treatment groups. FT, fibrous tissue; NB, native bone; RB, regenerated bone; *white arrow* represents defect margin; *white asterisks* represent ADM scaffold. Bright-field images obtained with 10× objective. Note osteointegration of bone at the defect margins across biopatterned growth factor therapy groups. Cement lines and reversal lines are present within the biopatterned growth factor therapy growth, depicting bone remodeling. Note the *purple staining* of lacunae with chondrocytes in **(B)** depicting endochondral ossification. Color images available online at www.liebertpub.com/tea

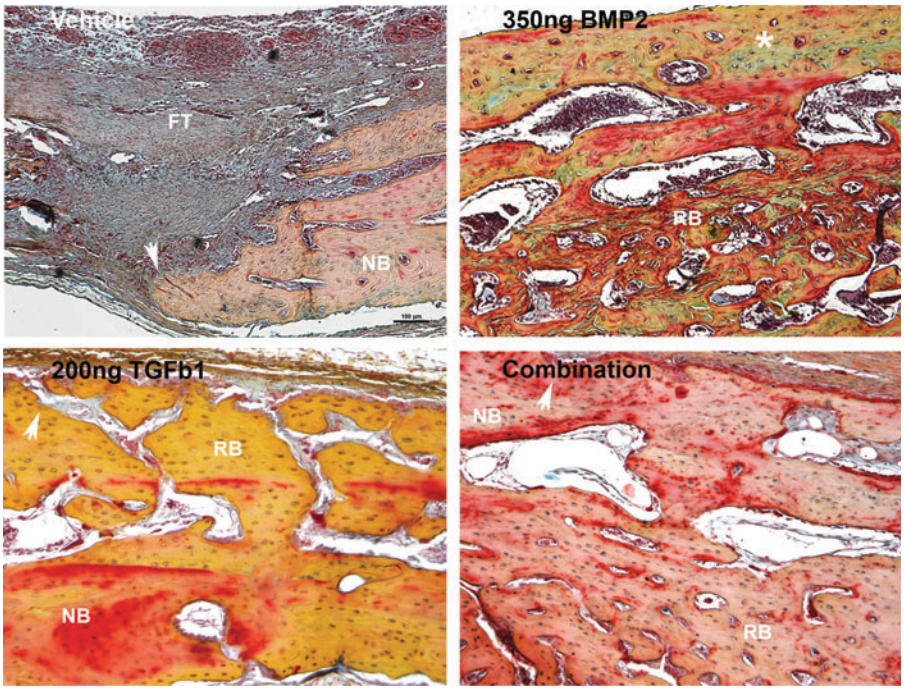

FIG. 7. Russell-Movat's Pentachrome composite of regenerated bone across treatment groups. FT, fibrous tissue; NB, native bone; RB, regenerated bone; *white arrow* represents defect margin; *white asterisk* represents endochondral ossification. Bright-field images obtained with 10×objective. Note the presence of endochondral ossification in the biopatterned BMP2-treated group, represented by a *green stain* (*white asterisk*). BMP2-regenerated bone was observed to contain more bone marrow spaces than bone regenerated in other treatment groups. *Yellow stain* represents immature woven bone. *Red stain* represents remodeled lamellar bone.

Gosain *et al.* suggest that linear 2D radiopaque defect closure may not accurately reflect 3D calvarial defect healing, consequently warranting cross-sectional analysis of the regenerated tissues.[60] Cross-sectional volumetric and density analysis mirrored the results obtained from the 2D defect closure analysis, suggesting that TGFβ1 and BMP2 are comparable osteoinductive agents in terms of quantitative outcomes. However, the densities of growth factor-regenerated bone were significantly less than native bone density, calling into question their functional utility.

Qualitatively, osteogenesis during the postsurgical period was consistent across all growth factor treatment groups as evidenced by visible cement lines and reversal lines and by the differential pentachrome staining of woven and lamellar bone. However, tissue morphology was distinct across treatment groups. Control and vehicle groups contained fibrous tissue spanning the entirety of the defect area with minimal bony islands present along the defect margins. Regenerated bone in the BMP2 treatment group appeared thicker than native bone with more marrow spaces. This regenerate contained lacunae with chondrocytes, suggestive of endochondral ossification. In contrast, calvarial bone normally forms through intramembranous ossification where mesenchymal cells condense and directly differentiate along

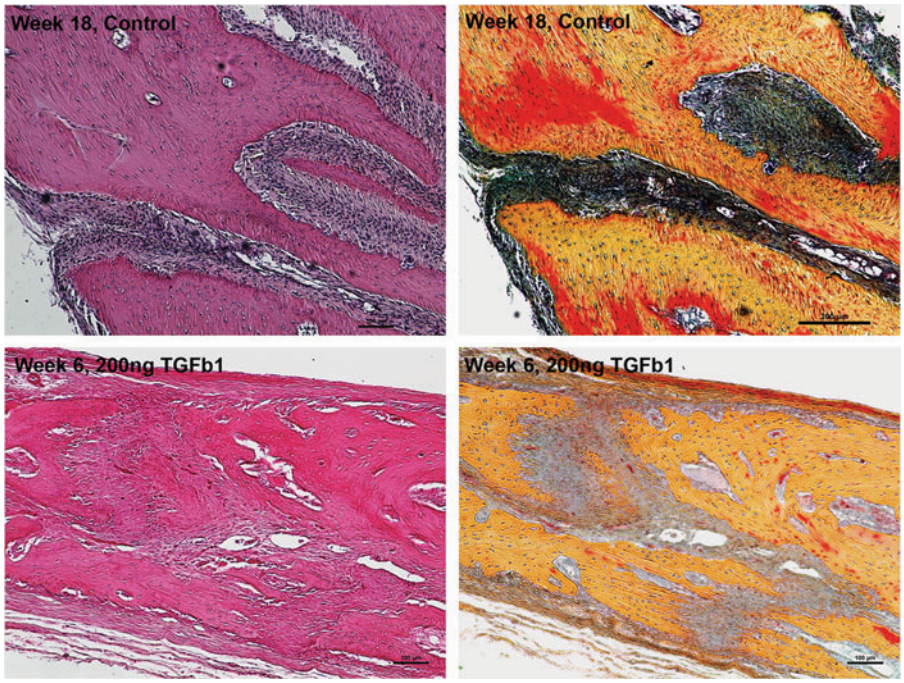

FIG. 8. Coronal suture regeneration in control and TGFβ1-treated groups. Bright-field H and E and pentachrome images obtained with 10× objective. Note regeneration of coronal suture in an 18-week-old control and in 6-week-old TGFβ1-treated rabbits. The neocoronal suture appears highly cellular and vascularized with interdigitating collagen fibers. Bone edges are maintained at a fixed distance with horizontally ordered osteoblasts lined along the neocoronal suture. Limited bone remodeling (*red stain*) is depicted in the 6-week-old TGFβ1-treated defect (*lower right panel*) as compared with remodeling in the 18-week-old control defect (*upper right panel*).

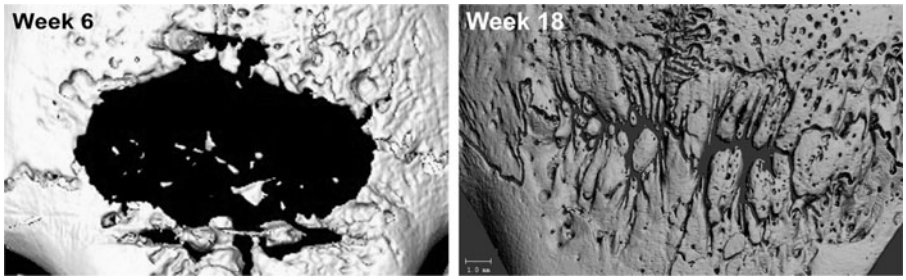

FIG. 9. Longitudinal control 2D defect healing assessed by CT imaging. Note the significant expansion of the day 10 defect area (3×15 mm strip) at week 6. The defect continues to heal at week 18 with noted sagittal and coronal suture regeneration.

an osteoblastic phenotype without a cartilage intermediate.[61] BMP2-regenerated bone appeared to regenerate bone along an ossification pathway foreign to native calvarial tissue. TGFβ1-regenerated bone appeared most similar to native bone in terms of matrix density and cellularity. There was no observed cartilage present, suggesting that TGFβ1-treated defects regenerated bone through the native intramembranous pathway. We hypothesize that the addition of TGFβ1 in the defect allowed for intramembranous bone formation, as combination growth factor therapy also lacked the presence of a cartilaginous intermediate to suggest endochondral ossification. There is significant clinical utility in regenerating membranous versus endochondral bone in the calvarial defect. Previous studies and clinical observations suggest that membranous bone grafted in the craniofacial region undergoes significantly less resorption when compared with endochondral bone.[62–65] Consequently, it becomes increasingly important for tissue-engineered calvarial bone to mimic the native architecture of the craniofacial skeleton.

Suture regeneration was observed in two groups. Control defects in 18-week-old rabbits and TGFβ1-treated defects in 6-week-old rabbits appeared to regenerate previously extirpated sutures. Moss previously defined a newly forming calvarial suture as a three-layered highly vascularized tissue comprising interdigitating collagen fibers that maintain a fixed distance between newly formed bone edges.[66] The regenerated control suture at 18 weeks of age appeared histologically equivalent to the TGFβ1-regenerated suture at 6 weeks of age. The functional importance of cranial sutures in the pediatric population cannot be overstated. These sutures serve as the major site for intramembranous bone growth and postnatal craniofacial growth, distribute mechanical forces across the calvaria, and allow for coordinated growth of the cranial vault with the expanding neurocranium.[67,68] Substantiating previous findings by Babler and Persing,[68] suture release, which was our surgical intervention, modulated cranial growth through significant defect expansion in control rabbits at 6 weeks of age.

Ideally, a tissue engineering approach to pediatric calvarial defect healing would allow for regeneration of soft (suture) and hard (bone) tissues to facilitate continued craniofacial growth and obviate the need for morbid autogenous bone grafting. Given the deleterious effects of suture fusion and endochondral ossification in this model, BMP2 therapy does not appear to be the most appealing therapy. Clinically, and in many animal models, rhBMP2-based craniofacial reconstructions involve supraphysiologic doses on the order of milligrams.[69–72] Our model utilized 350 ng of BMP2, yet this low dose still superseded native calvarial defect healing mechanisms by fusing sutures and regenerating bone through a cartilaginous intermediate. In this model, TGFβ1 therapy significantly augmented bony defect healing at an earlier time point when compared with control, regenerated bone along the native intramembranous ossification pathway, and (unlike BMP2 alone or in combination with TGFβ1) permitted normal suture reformation. Contrary to our initial hypothesis, we did not observe increased bone formation or suture reformation with combination growth factor therapy of BMP2 and TGFβ1. Limitations of this study include the use of single-dose growth factors, use of a juvenile rabbit model, and analysis at a single postoperative time point.

The data obtained from this study highlight the need for a shift in tissue engineering outcomes analysis. Often, the main outcome measure of calvarial tissue engineering is simply radiopaque coverage of the calvarial defect. Although recent advances in tissue engineering allow for the complete coverage of these large bony defects, existing studies have not systematically elucidated the quality, quantity, and interaction of regenerated tissues within their native substratum. Thorough evaluation of regenerated tissues becomes increasingly critical as these tissues interact with native tissues as part of the functional matrix of a growing craniofacial skeleton. Tissue engineers must consider regenerated tissue biology and the pathways through which these tissues develop to design more effective and comprehensive therapies.

Disclosure Statement

No competing financial interests exist.

References

1. Hanson, J.W., *et al.* Subtotal neonatal calvariectomy for severe craniosynostosis. J Pediatr **91,** 257, 1977.
2. Mabbutt, L.W., and Kokich, V.G. Calvarial and sutural redevelopment following craniectomy in the neonatal rabbit. J Anat **129(Pt 2),** 413, 1979.
3. Mabbutt, L.W., *et al.* Subtotal neonatal calvariectomy. A radiographic and histological evaluation of calvarial and sutural redevelopment in rabbits. J Neurosurg **51,** 691, 1979.
4. Sirola, K. Regeneration of defects in the calvaria. An experimental study. Ann Med Exp Biol Fenn **38(Suppl 2),** 1, 1960.
5. Reid, C.A., McCarthy, J.G., and Kolber, A.B. A study of regeneration in parietal bone defects in rabbits. Plast Reconstr Surg **67,** 591, 1981.
6. Mossaz, C.F., and Kokich, V.G. Redevelopment of the calvaria after partial craniectomy in growing rabbits: the effect of altering dural continuity. Acta Anat (Basel) **109,** 321, 1981.

7. Wan, D.C., *et al.* Differential gene expression between juvenile and adult dura mater: a window into what genes play a role in the regeneration of membranous bone. Plast Reconstr Surg **118,** 851, 2006.
8. Greene, A.K., *et al.* Pediatric cranioplasty using particulate calvarial bone graft. Plast Reconstr Surg **122,** 563, 2008.
9. Koenig, W.J., Donovan, J.M., and Pensler, J.M. Cranial bone grafting in children. Plast Reconstr Surg **95,** 1, 1995.
10. Inoue, A., *et al.* Cranioplasty with split-thickness calvarial bone. Neurol Med Chir (Tokyo) **35,** 804, 1995.
11. Cho, Y.R., and Gosain, A.K. Biomaterials in craniofacial reconstruction. Clin Plast Surg **31,** 377; v, 2004.
12. De Long, W.G., Jr., *et al.* Bone grafts and bone graft substitutes in orthopaedic trauma surgery. A critical analysis. J Bone Joint Surg Am **89,** 649, 2007.
13. Arnaud, E., *et al.* Osteogenesis with coral is increased by BMP and BMC in a rat cranioplasty. Biomaterials **20,** 1909, 1999.
14. Cowan, C.M., *et al.* Bone morphogenetic protein 2 and retinoic acid accelerate in vivo bone formation, osteoclast recruitment, and bone turnover. Tissue Eng **11,** 645, 2005.
15. Cowan, C.M., *et al.* Adipose-derived adult stromal cells heal critical-size mouse calvarial defects. Nat Biotechnol **22,** 560, 2004.
16. Dudas, J.R., *et al.* The osteogenic potential of adipose-derived stem cells for the repair of rabbit calvarial defects. Ann Plast Surg **56,** 543, 2006.
17. Hollinger, J., *et al.* Calvarial bone regeneration using osteogenin. J Oral Maxillofac Surg **47,** 1182; discussion 1187, 1989.
18. Lindholm, T.C., *et al.* Bovine bone morphogenetic protein (bBMP/NCP)-induced repair of skull trephine defects in pigs. Clin Orthop Relat Res 263, 1994.
19. Ripamonti, U., *et al.* Osteogenin, a bone morphogenetic protein, adsorbed on porous hydroxyapatite substrata, induces rapid bone differentiation in calvarial defects of adult primates. Plast Reconstr Surg **90,** 382, 1992.
20. Sato, K., and Urist, M.R. Induced regeneration of calvaria by bone morphogenetic protein (BMP) in dogs. Clin Orthop Relat Res 301, 1985.
21. Sheehan, J.P., *et al.* The safety and utility of recombinant human bone morphogenetic protein-2 for cranial procedures in a nonhuman primate model. J Neurosurg **98,** 125, 2003.
22. Wozney, J.M., *et al.* Novel regulators of bone formation: molecular clones and activities. Science **242,** 1528, 1988.
23. Ripamonti, U., *et al.* Complete regeneration of bone in the baboon by recombinant human osteogenic protein-1 (hOP-1, bone morphogenetic protein-7). Growth Factors **13,** 273; color plates III–VIII, pre bk, 1996.
24. Carstens, M. Clinical applications of recombinant human bone morphogenetic protein in craniofacial surgery. In: International Society of Craniofacial Surgery. Bahia, Brazil, 2007.
25. J., B. Panel 2: bone morphogenetic proteins. In: International Society of Craniofacial Surgery. Bahia, Brazil, 2007.
26. Podda, S.A.W., SA. Switch cranioplasty and BMP-2 in a hemicranial reconstruction in an infant. In: International Society of Craniofacial Surgery. Bahia, Brazil, 2007.
27. Garrett, M.P., *et al.* Formation of painful seroma and edema after the use of recombinant human bone morphogenetic protein-2 in posterolateral lumbar spine fusions. Neurosurgery **66,** 1044; discussion 1049, 2010.
28. Lehman, R.A., Jr., and Kang, D.G. Symptomatic ectopic intracanal ossification after transforaminal lumbar interbody fusion with rhBMP-2. Spine J **12,** 530, 2012.
29. Shah, R.K., *et al.* Recombinant human bone morphogenetic protein 2-induced heterotopic ossification of the retroperitoneum, psoas muscle, pelvis and abdominal wall following lumbar spinal fusion. Skeletal Radiol **39,** 501, 2010.
30. Smucker, J.D., *et al.* Increased swelling complications associated with off-label usage of rhBMP-2 in the anterior cervical spine. Spine (Phila Pa 1976) **31,** 2813, 2006.
31. Kinsella, C.R., Jr., *et al.* Recombinant human bone morphogenetic protein-2-induced craniosynostosis and growth restriction in the immature skeleton. Plast Reconstr Surg **127,** 1173, 2011.
32. Arnander, C., *et al.* Three-dimensional technology and bone morphogenetic protein in frontal bone reconstruction. J Craniofac Surg **17,** 275, 2006.
33. Oetgen, M.E., and Richards, B.S. Complications associated with the use of bone morphogenetic protein in pediatric patients. J Pediatr Orthop **30,** 192, 2010.
34. Woo, E.J. Adverse events after recombinant human BMP2 in nonspinal orthopaedic procedures. Clin Orthop Relat Res **471,** 1707, 2013.
35. Carragee, E.J., Hurwitz, E.L., and Weiner, B.K. A critical review of recombinant human bone morphogenetic protein-2 trials in spinal surgery: emerging safety concerns and lessons learned. Spine J **11,** 471, 2011.
36. Lindley, T.E., *et al.* Complications associated with recombinant human bone morphogenetic protein use in pediatric craniocervical arthrodesis. J Neurosurg Pediatr **7,** 468, 2011.
37. Zara, J.N., *et al.* High doses of bone morphogenetic protein 2 induce structurally abnormal bone and inflammation in vivo. Tissue Eng Part A **17,** 1389, 2011.
38. Beck, L.S., *et al.* In vivo induction of bone by recombinant human transforming growth factor beta 1. J Bone Miner Res **6,** 961, 1991.
39. Tanaka, T., *et al.* Morphological study of recombinant human transforming growth factor beta 1-induced intramembranous ossification in neonatal rat parietal bone. Bone **14,** 117, 1993.
40. Celeste, A.J., *et al.* Identification of transforming growth factor beta family members present in bone-inductive protein purified from bovine bone. Proc Natl Acad Sci U S A **87,** 9843, 1990.
41. Ripamonti, U., *et al.* Transforming growth factor-beta isoforms and the induction of bone formation: implications for reconstructive craniofacial surgery. J Craniofac Surg **20,** 1544, 2009.
42. Vehof, J.W., *et al.* Bone formation in transforming growth factor beta-1-coated porous poly(propylene fumarate) scaffolds. J Biomed Mater Res **60,** 241, 2002.
43. Cooper, G.M., *et al.* Inkjet-based biopatterning of bone morphogenetic protein-2 to spatially control calvarial bone formation. Tissue Eng Part A **16,** 1749, 2010.
44. Manning, P.J., Ringler, D.H., and Newcomer, C.E. The Biology of the Laboratory Rabbit, 2nd edition. American College of Laboratory Animal Medicine series. San Diego: Academic Press, 1994, xiii, p. 483.
45. Frazier, B.C., *et al.* Comparison of craniofacial phenotype in craniosynostotic rabbits treated with anti-Tgf-beta2 at suturectomy site. Cleft Palate Craniofac J **45,** 571, 2008.
46. Sahoo, N.K., and Rangan, M. Role of split calvarial graft in reconstruction of craniofacial defects. J Craniofac Surg **23,** e326, 2012.
47. Chen, D., Zhao, M., and Mundy, G.R. Bone morphogenetic proteins. Growth Factors **22,** 233, 2004.

48. Ebendal, T., Bengtsson, H., and Soderstrom, S. Bone morphogenetic proteins and their receptors: potential functions in the brain. J Neurosci Res **51,** 139, 1998.
49. Fukuda, S., and Taga, T. Cell fate determination regulated by a transcriptional signal network in the developing mouse brain. Anat Sci Int **80,** 12, 2005.
50. Furuta, Y., Piston, D.W., and Hogan, B.L. Bone morphogenetic proteins (BMPs) as regulators of dorsal forebrain development. Development **124,** 2203, 1997.
51. Goldstein, A.M., *et al.* BMP signaling is necessary for neural crest cell migration and ganglion formation in the enteric nervous system. Mech Dev **122,** 821, 2005.
52. Knosp, W.M., *et al.* HOXA13 regulates the expression of bone morphogenetic proteins 2 and 7 to control distal limb morphogenesis. Development **131,** 4581, 2004.
53. Lincoln, J., Alfieri, C.M., and Yutzey, K.E. BMP and FGF regulatory pathways control cell lineage diversification of heart valve precursor cells. Dev Biol **292,** 292, 2006.
54. Mabie, P.C., Mehler, M.F., and Kessler, J.A. Multiple roles of bone morphogenetic protein signaling in the regulation of cortical cell number and phenotype. J Neurosci **19,** 7077, 1999.
55. Machingo, Q.J., Fritz, A., and Shur, B.D. A beta1,4-galactosyltransferase is required for Bmp2-dependent patterning of the dorsoventral axis during zebrafish embryogenesis. Development **133,** 2233, 2006.
56. Nilsson, O.S., and Urist, M.R. Immune inhibition of repair of canine skull trephine defects implanted with partially purified bovine morphogenetic protein. Int Orthop **15,** 257, 1991.
57. Urist, M.R., *et al.* Osteoporosis: a bone morphogenetic protein auto-immune disorder. Prog Clin Biol Res **187,** 77, 1985.
58. Zhang, D., *et al.* Development of bone morphogenetic protein receptors in the nervous system and possible roles in regulating trkC expression. J Neurosci **18,** 3314, 1998.
59. Persson, K.M., *et al.* Craniofacial growth following experimental craniosynostosis and craniectomy in rabbits. J Neurosurg **50,** 187, 1979.
60. Gosain, A.K., *et al.* Osteogenesis in cranial defects: reassessment of the concept of critical size and the expression of TGF-beta isoforms. Plast Reconstr Surg **106,** 360; discussion 372, 2000.
61. Chung, U.I., *et al.* Distinct osteogenic mechanisms of bones of distinct origins. J Orthop Sci **9,** 410, 2004.
62. Smith, J.D., and Abramson, M. Membranous vs endochondrial bone autografts. Arch Otolaryngol **99,** 203, 1974.
63. Ferraro, J.W. Experimental evaluation of ceramic calcium phosphate as a substitute for bone grafts. Plast Reconstr Surg **63,** 634, 1979.
64. Holmes, R.E. Bone regeneration within a coralline hydroxyapatite implant. Plast Reconstr Surg **63,** 626, 1979.
65. Zins, J.E., and Whitaker, L.A. Membranous versus endochondral bone: implications for craniofacial reconstruction. Plast Reconstr Surg **72,** 778, 1983.
66. Moss, M.L. Experimental alteration of sutural area morphology. Anat Rec **127,** 569, 1957.
67. Opperman, L.A. Cranial sutures as intramembranous bone growth sites. Dev Dyn **219,** 472, 2000.
68. Babler, W.J., and Persing, J.A. Experimental alteration of cranial suture growth: effects on the neurocranium, basicranium, and midface. Prog Clin Biol Res **101,** 333, 1982.
69. Carstens, M.H., Chin, M., and Li, X.J. In situ osteogenesis: regeneration of 10-cm mandibular defect in porcine model using recombinant human bone morphogenetic protein-2 (rhBMP-2) and Helistat absorbable collagen sponge. J Craniofac Surg **16,** 1033, 2005.
70. Carstens, M.H., *et al.* Reconstruction of #7 facial cleft with distraction-assisted in situ osteogenesis (DISO): role of recombinant human bone morphogenetic protein-2 with Helistat-activated collagen implant. J Craniofac Surg **16,** 1023, 2005.
71. Chao, M., *et al.* In situ osteogenesis of hemimandible with rhBMP-2 in a 9-year-old boy: osteoinduction via stem cell concentration. J Craniofac Surg **17,** 405, 2006.
72. Chin, M., *et al.* Repair of alveolar clefts with recombinant human bone morphogenetic protein (rhBMP-2) in patients with clefts. J Craniofac Surg **16,** 778, 2005.

Address correspondence to:
Gregory M. Cooper, PhD
Department of Plastic Surgery
Craniofacial Biology Laboratory
Children's Hospital of Pittsburgh of UPMC
3510 Rangos Research Center
4401 Penn Avenue
Pittsburgh, PA 15224

E-mail: greg.cooper@chp.edu

Received: April 5, 2014
Accepted: October 3, 2014
Online Publication Date: February 4, 2015